

Synthesis of TiO₂ Photoelectrode Nanostructures for Sensing and Removing Textile Compounds Rhodamine B

Zul Arham^{1,*}, Kurniawan Kurniawan², Ismaun Ismaun¹

¹ Department of Mathematics and Natural Sciences, Faculty of Tarbiyah, Institut Agama Islam Negeri (IAIN) Kendari, 93116, Southeast Sulawesi, Indonesia

² Department of Textile Chemistry, Politeknik STTT Bandung, 40272, West Java, Indonesia

* Correspondence: arhamzul88@yahoo.com (Z.A.);

Scopus Author ID 57195056274

Received: 8.07.2021; Revised: 30.08.2021; Accepted: 4.09.2021; Published: 19.10.2021

Abstract: The study of the sensing and removal of Rhodamine B (RhB) textile compounds is the photoelectrocatalytic system applications development. RhB was used as a model to study the performance of TiO₂ (NTiO₂) photoelectrode nanostructures as environmentally friendly sensors. The synthesis of NTiO₂ was carried out on the surface of the Titanium electrode by applying a potential bias of 25.0 V. The NTiO₂ formed on the surface of the Titanium electrode (NTiO₂/Ti) was characterized using SEM, XRD, FTIR, and Cyclic Voltammetry (CV). The formation of NTiO₂ is characterized by the formation of a honeycomb-like tube on the Ti electrode surface. In addition, it is strengthened by diffractogram peaks at $2\theta = 25^\circ$ and 48° and IR absorption at wavenumbers of 3441.01 cm^{-1} (-OH groups) and 1629.85 cm^{-1} (Ti-O group). As for the results of sensing RhB using CV, it is known that RhB is oxidized on the surface of NTiO₂/Ti with a value of $E_a = 1.54\text{ V}$. The oxidation process that occurs is controlled by the diffusion rate. Based on the results of photoelectrocatalytic RhB removal for 60 minutes, it was shown that using 0.10 M NaCl support electrolyte effectively increased the RhB removal rate. The decrease in RhB concentration during the photoelectrocatalytic removal process was 74.21%.

Keywords: NTiO₂; Ti electrode; Rhodamine B; photoelectrocatalytic system; oxide potential.

© 2021 by the authors. This article is an open-access article distributed under the terms and conditions of the Creative Commons Attribution (CC BY) license (<https://creativecommons.org/licenses/by/4.0/>).

1. Introduction

Textile compound waste has been an aquatic environmental issue for many years. The complex and stable structure is a major problem in the processing and recycling process [1–3]. Many methods have been developed, and their performance reported in dealing with this problem is the photoelectrocatalytic method. This method is an advanced technology that has attracted the attention of many researchers in the last decade, which is specifically studied in the release of organic pollutants in the aquatic environment [4]. In addition, the photoelectrocatalytic method is used as an alternative method to overcome the weaknesses of the photocatalytic method [5]. The application of this method is carried out through a redox mechanism on the surface of the photoelectrode known as the photoanode [5, 6].

In the development of photoelectrocatalytic methods, TiO₂ has been extensively studied and applied as a photoelectrode [1, 7]. The advantages of TiO₂ as a photoelectrode include environmental friendliness [8, 9], high oxidizing power [10], low cost [11], non-toxic [12], and good photocatalytic activity [13]. However, some disadvantages of TiO₂ have also been reported, such as the fast electron (e^-) and hole (h^+) recombination rates [14]. The

recombination phenomenon causes the performance of TiO₂ photoelectrodes in various applications to be reduced. Based on this problem, TiO₂ has been modified a lot. The reported modifications include doping with metal conductors such as Ag [14–16], Au [17], and Pt [18], doping of semiconductor oxide materials such as WO₃ [19], SiO₂ [20, 21], V₂O₅ [22] and Bi₂O₃ [23], and doping with organic compounds [24]. Another modification that has also attracted much attention is the modification of the shape of the surface structure of TiO₂, such as barrier-layer [25], mesoporous [26], nanopores [27], and nanotubes [2].

This study examines the performance of TiO₂ photoelectrodes whose surface structure is modified into nanotubes. Modifying the surface structure of TiO₂ photoelectrodes into nanotubes has been reported to be effective in reducing the rate of e^- and h^+ recombination, thereby helping to improve the performance of TiO₂ photoelectrodes [28]. The obtained NTiO₂ photoelectrodes were then applied for photoelectrocatalytic sensing and removal of RhB. The fundamental difference between this study and previous studies is the application of potential bias in the e^- exciting flow to the external circuit of the photoelectrocatalytic system, where the potential bias used is derived from the RhB sensing information on the surface of the NTiO₂ photoelectrode. In addition to overcoming the problem of TiO₂ photoelectrode recombination, this effort can be used as a preliminary study for the application of TiO₂ photoelectrodes in the field of sensors and biosensors by photoelectrocatalysis. This application has been reported by [29–31].

2. Materials and Methods

2.1. NTiO₂ photoelectrode synthesis.

NTiO₂ photoelectrode synthesis was carried out based on the results of the research reported by [1]. In summary, the Ti and Cu electrodes ($\pm 4 \times 0.70$ cm) were cleaned with ethanol solution. Then the two electrodes were placed into a container (anodizing cell) containing a solution of 87 % glycerol, 0.27 M NH₄F, and 4 mL of distilled water. The Ti electrode is placed as the anode, and Cu is placed as the cathode. The formation of TiO₂ nanotubes was carried out for 4 hours at a potential of 25.0 V. The NTiO₂ photoelectrodes were rinsed with distilled water, dried in the open air, and heated at 500 °C for 3 hours. Characterization process using SEM, XRD, and FTIR.

2.2. Sensing RhB using NTiO₂.

The RhB sensing process was carried out using a cyclic voltammetry technique using an eDAC Potentiostat by adopting the procedure reported by [32,33]. The NTiO₂ photoelectrode was placed as the working electrode, while Ag/AgCl and Pt wire were placed as a reference and auxiliary electrodes, respectively. The three electrodes were inserted into a voltammetry cell containing 0.0001 M rhodamine B solution and a phosphate buffer supporting electrolytes of pH 4, 7, and 10. The sensing process was carried out at a potential range of -1.2 to +1.8 V with a scan rate of 100 mV/s.

2.3. Photoelectrocatalytic RhB removal.

Photoelectrocatalytic removal of RhB was carried out in a UV reactor with 2 electrodes. The NTiO₂ photoelectrode was placed as the anode and the Pt wire as the cathode. The photoelectrode and Pt wire are connected to a DC power supply (GW Instek GPS 30300) and

are biased at 1.50 V (RhB sensing potential). During the discharge process, magnetic stirring was carried out at room temperature. Changes in the concentration of RhB were measured at $\lambda_{\text{max}} = 540 \text{ nm}$ using Agilent 8453 UV-Vis Spectrophotometer. In the photoelectrocatalytic removal process, testing was carried out on the type of supporting electrolyte and the different removal methods (photodegradation, electrochemical and photocatalytic) as a comparison. The RhB used in the study was purchased from Sigma-Aldrich. The initial RhB concentration tested was 1.20 ppm.

3. Results and Discussion

3.1. Characterization of SEM, XRD, and FTIR.

Figure 1A shows the results of the SEM characterization of the NTiO₂ photoelectrode. These results show the formation of a honeycomb-like tube that is evenly distributed on the surface of the photoelectrode. Honeycomb is a hallmark of the successful modification of the TiO₂ nanostructure photoelectrode modification process [13]. Another feature of the successful manufacture of NTiO₂ photoelectrodes was observed using XRD and FTIR. Based on XRD analysis (Figure 1B), the success of making NTiO₂ photoelectrodes was observed by the appearance of diffractogram peaks at $2\theta = 25^\circ$ and 48° [34–36]. This peak is reported as a typical peak for anatase TiO₂. This result is corroborated by the IR absorption peaks (Figure 1C) at wavenumbers 3441.01 cm^{-1} and 1629.85 cm^{-1} which are absorptions for the -OH and Ti-O groups, respectively [37, 38].

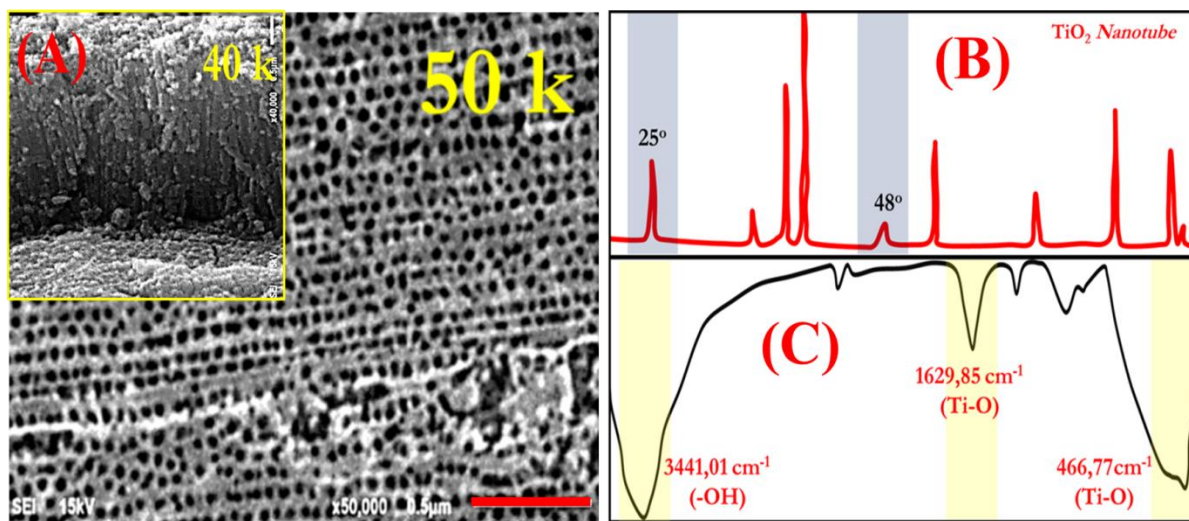


Figure 1. Characterization of NTiO₂ photoelectrode : (A) SEM, (B) XRD, and (C) FTIR.

3.2. Sensing RhB using photoelectrode TiO₂.

Figure 2 shows the cyclic voltammogram of the RhB oxidation on the surface of the NTiO₂ photoelectrode. RhB was oxidized at a potential value of 1.54 V (Figure 2A). This oxidation process occurs in the use of a phosphate buffer supporting electrolyte pH 4.0. Based on the voltammogram, it can be seen that there is an effect of pH on the oxidation of RhB on the surface of the NTiO₂ photoanode. The RhB oxidation at pH 4.0 was corroborated by the absence of an oxidation peak when measurements were made in the supporting electrolyte solution (Figure 2B). In addition, the RhB oxidation process was strengthened by testing for variations in RhB concentrations (Figure 2C). The result is that there is a linear relationship

between concentration and peak oxidation state of RhB. This potential oxidation value is then used during the photoelectrocatalytic release of RhB.

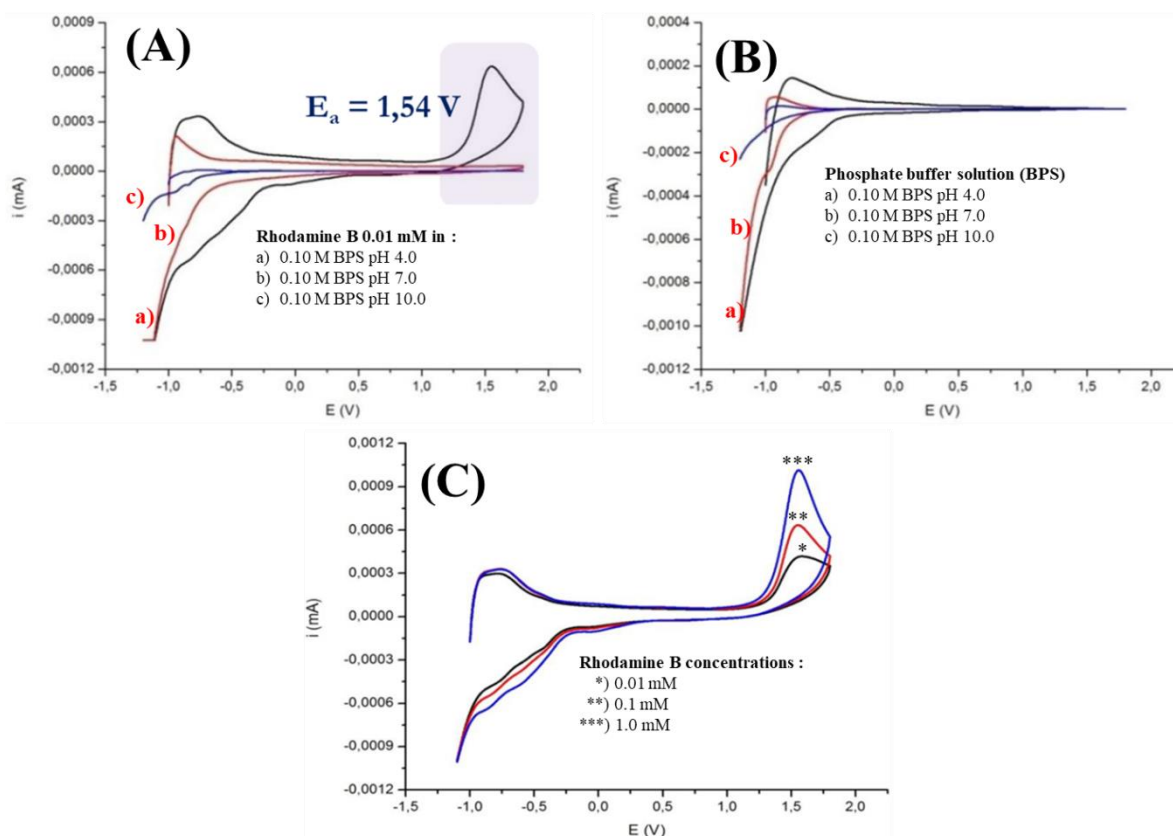


Figure 2. Cyclic voltammogram of RhB on the surface of the NTiO₂ photoelectrode : (A) based on variations in the pH of the electrolyte solution; (B) in a supporting electrolyte solution; and (C) based on variations in RhB concentration.

3.3. Photoelectrocatalytic removal of RhB.

The photoelectrocatalytic removal of RhB using NTiO₂ photoelectrodes was initiated by studying the effect of the electrolyte solution type. In addition to helping increase the current, some electrolyte solutions are reported to be able to initiate the formation of radical compounds that will accelerate the degradation process. Figure 3A shows the effect of using a supporting electrolyte on the release of RhB. The highest release percentage (% release) was produced in a solution containing 0.1 M NaCl, which was 62.50%. These results became the basis for selecting 0.1 M NaCl as an electrolyte solution during the RhB release process. Cl⁻ ions will significantly reduce the number of RhB molecules in the solution. Cl⁻ ions will also migrate to the surface of NTiO₂ photoelectrode and can be adsorbed and converted by electron-hole pairs (e^-/h^+) into groups with high oxidizing activity, such as Cl^{*}, and Cl₂. The oxidizing species then help to oxidize the organic compounds. Figure 3B shows the performance of the four tested methods in the RhB removal process. These methods include photodegradation (PD), electrochemical (EC), photocatalytic (PC), and photoelectrocatalytic (PEC). Compared to the other three methods, PEC showed the best release performance with a % release of 74.21%. The success strongly influences this result in making NTiO₂ photoelectrodes, where the final result of this process is shown in Figure 3C.

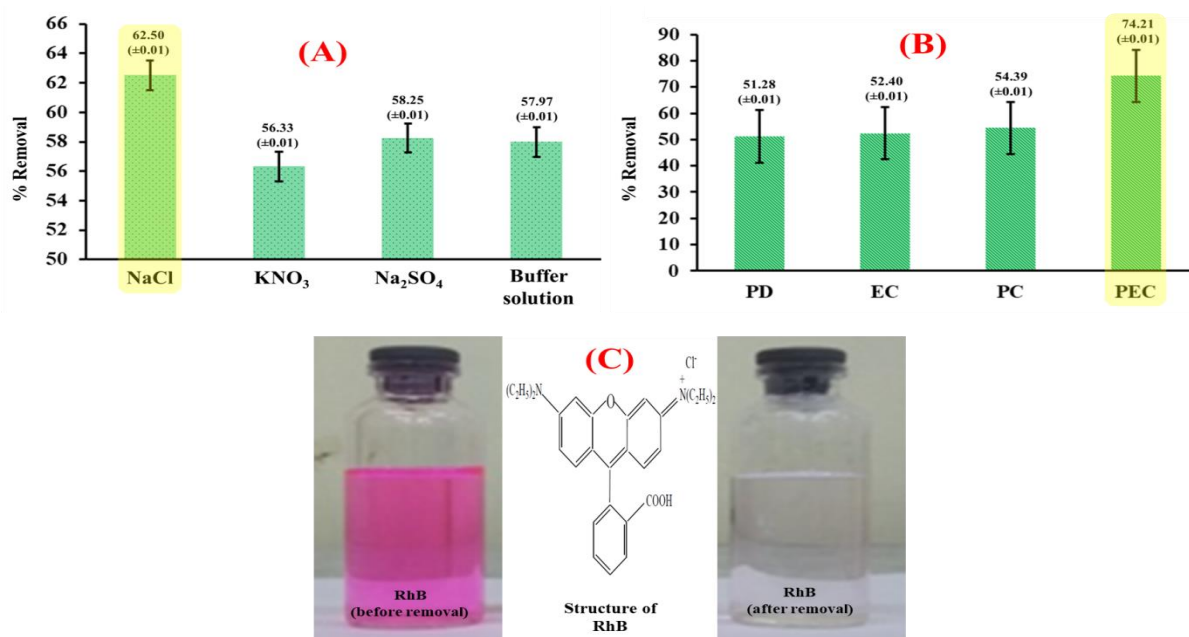


Figure 4. (A) the performance of various electrolyte solutions; (B) the performance of various removal methods; (C) the final product of the RhB photoelectrocatalytic removal.

4. Conclusions

The study on the application of NTiO₂ photoelectrodes in photoelectrocatalytic sensing and removal showed good performance for removing Rhodamine B textile waste. The use of electrochemical methods in the synthesis of photoelectrodes succeeded in changing the surface structure of TiO₂ into nanotubes. This condition makes photoelectrocatalytic removal more effective than other removal systems such as photodegradation, electrochemistry, and photocatalysis. The % removal resulting from the application of the NTiO₂ photoelectrode in the RhB removal for 60 minutes was 74.21%. Another result of this study shows that the supporting electrolyte strongly influences the photoelectrocatalytic removal system, wherein NaCl shows better performance as the supporting electrolyte. Overall, this study shows that the photoelectrocatalytic removal system with oxidation potential shows good potential to be studied more extensively in the future.

Funding

This research was conducted through independent funding from the author.

Acknowledgment

This research has no acknowledgment.

Conflicts of Interest

We declare that this article has no conflict of interest.

References

- Zul, A.; Muhammad, N.; Buchari, B. Photoelectrocatalysis performance of La₂O₃ doped TiO₂/Ti electrode in degradation of rhodamine B organic compound. *International journal of chemtech research* **2016**, *9*, 113–130.
- Montenegro-Ayo, R.; Morales-Gomero, J.C.; Alarcon, H.; Corzo, A.; Westerhoff, P.; Garcia-Segura, S.

- Photoelectrocatalytic degradation of 2, 4-dichlorophenol in a TiO₂ nanotube-coated disc flow reactor. *Chemosphere* **2021**, 268, 129320, <https://doi.org/10.1016/j.chemosphere.2020.129320>.
3. Muzakkar, M.Z.; Natsir, M.; Alisa, A.; Maulidiyah, M.; Salim, L.O.A.; Sulistiyani, I.; Nurdin, M. Photoelectrocatalytic degradation of reactive red 141 using FeTiO₃ composite doped TiO₂/Ti electrodes. In *Journal of Physics: Conference Series. IOP Publishing* **2021**, 1899, 12043, <https://doi.org/10.1088/1742-6596/1899/1/012043>.
 4. Wibowo, D.; Muzakkar, M.Z.; Maulidiyah, M.; Nurdin, M.; Saad, S.K.M.; Umar, A.A. Morphological Analysis of Ag Doped on TiO₂/Ti Prepared via Anodizing and Thermal Oxidation Methods. *Biointerface Research in Applied Chemistry* **2021**, 12, 1421-1427, <https://doi.org/10.33263/BRIAC122.14211427>.
 5. Wang, Y.; Zu, M.; Zhou, X.; Lin, H.; Peng, F.; Zhang, S. Designing efficient TiO₂-based photoelectrocatalysis systems for chemical engineering and sensing. *Chemical Engineering Journal* **2020**, 381, 122605, <https://doi.org/10.1016/j.cej.2019.122605>.
 6. Palmas, S.; Mais, L.; Mascia, M.; Vacca, A. Trend in using TiO₂ nanotubes as photoelectrodes in PEC processes for wastewater treatment. *Current Opinion in Electrochemistry* **2021**, 28, 100699, <https://doi.org/10.1016/j.coelec.2021.100699>.
 7. Brüger, A.; Fafilek, G.; Neumann-Spallart, M. Treatment of cyanide: Photoelectrocatalytic degradation using TiO₂ thin film electrodes and influence of volatilization. *Solar Energy*, **2020**, 205, 74-78, <https://doi.org/10.1016/j.solener.2020.05.035>.
 8. Maulidiyah, M.; Azis, T.; Lindayani, L.; Wibowo, D.; Salim, L.O.A.; Aladin, A.; Nurdin, M. Sol-gel TiO₂/Carbon Paste Electrode Nanocomposites for Electrochemical-assisted Sensing of Fipronil Pesticide. *Journal of Electrochemical Science and Technology* **2019**, 10, 394-401, <https://doi.org/10.33961/jecst.2019.00178>.
 9. Nurdin, M.; Prabowo, O.A.; Arham, Z.; Wibowo, D.; Maulidiyah, M.; Saad, S.K.M.; Umar, A.A. Highly sensitive fipronil pesticide detection on ilmenite (FeO. TiO₂)-carbon paste composite electrode. *Surfaces and Interfaces* **2019**, 16, 108-113, <https://doi.org/10.1016/j.surfin.2019.05.008>.
 10. Maulidiyah; Azis, T.; Nurwahidah, A.T.; Wibowo, D.; Nurdin, M. Photoelectrocatalyst of Fe co-doped N-TiO₂/Ti nanotubes: pesticide degradation of thiamethoxam under UV-visible lights. *Environmental nanotechnology, monitoring & management* **2017**, 8, 103-111, <https://doi.org/10.1016/j.enmm.2017.06.002>.
 11. Nurdin, M.; Muzakkar, M.Z.; Maulidiyah, M.; Maulidiyah, N.; Wibowo, D. Plasmonic silver-N/TiO₂ effect on photoelectrocatalytic oxidation reaction. *J Mater Env. Sci* **2016**, 7, 3334-3343.
 12. Maulidiyah, M.; Susilowati, P.E.; Mudhafar, N.K.; Arham, Z.; Nurdin, M. Photo-Inactivation Staphylococcus aureus by Using Formulation of Mn-N-TiO₂ Composite Coated Wall Paint. *Biointerface Research in Applied Chemistry* **2021**, 12, 1628-1637, <https://doi.org/10.33263/BRIAC122.16281637>.
 13. Wibowo, D.; Muzakkar, M. Z.; Saad, S.K.M.; Mustapa, F.; Maulidiyah, M.; Nurdin, M.; Umar, A.A. Enhanced visible light-driven photocatalytic degradation supported by Au-TiO₂ coral-needle nanoparticles. *Journal of Photochemistry and Photobiology A: Chemistry* **2020**, 398, 112589, <https://doi.org/10.1016/j.jphotochem.2020.112589>.
 14. Teng, W.; Xu, J.; Cui, Y.; Yu, J. Photoelectrocatalytic degradation of sulfadiazine by Ag₃PO₄/MoS₂/TiO₂ nanotube array electrode under visible light irradiation. *Journal of Electroanalytical Chemistry* **2020**, 868, 114178, <https://doi.org/10.1016/j.jelechem.2020.114178>.
 15. Lopez, E.C.R.; Cleofe, V.A.F.; Cañal, R.Y.A.; Boado, K.F.P.; Perez, J.V.D. Photoelectrocatalytic Degradation of CI Basic Blue 9 under UV Light Using Silver-Doped Titanium Dioxide Nanotubes. *Key Engineering Materials* **2020**, 831, 132-141, <https://doi.org/10.4028/www.scientific.net/KEM.831.132>.
 16. Rajput, H.; Sangal, V.K.; Dhir, A. Synthesis of highly stable and efficient Ag loaded GO/TiO₂ nanotube electrodes for the photoelectrocatalytic degradation of pentachlorophenol. *Journal of Electroanalytical Chemistry* **2018**, 814, 118-126, <https://doi.org/10.1016/j.jelechem.2018.02.053>.
 17. Guo, H.; Su, C.; Zhang, Y.; Yu, D.; Li, L.; Liu, Z. Facile synthesis of TiO₂/PbS heterojunction with Au doped for photoelectrocatalytic degradation. *Materials Letters* **2020**, 264, 127371, <https://doi.org/10.1016/j.matlet.2020.127371>.
 18. Guaraldo, T.T.; De Brito, J.F.; Wood, D.; Zanoni, M.V.B. A new Si/TiO₂/Pt pn junction semiconductor to demonstrate photoelectrochemical CO₂ conversion. *Electrochimica Acta* **2015**, 185, 117-124, <https://doi.org/10.1016/j.electacta.2015.10.077>.
 19. Hunge, Y.M.; Mahadik, M. A.; Moholkar, A.V.; Bhosale, C.H. Photoelectrocatalytic degradation of oxalic acid using WO₃ and stratified WO₃/TiO₂ photocatalysts under sunlight illumination. *Ultrasonics sonochemistry* **2017**, 35, 233-242, <https://doi.org/10.1016/j.ultsonch.2016.09.024>.
 20. Fan, X.L.; Zhang, C.X.; Xue, H.R.; Guo, H.; Song, L.; He, J.P. Fabrication of SiO₂ incorporated ordered mesoporous TiO₂ composite films as functional Pt supports for photo-electrocatalytic methanol oxidation. *RSC advances* **2015**, 5, 78880-78888, <https://doi.org/10.1039/C5RA12810B>.
 21. Liu, Y.; Yu, H. Lv, Z.; Zhan, S.; Yang, J.; Peng, X.; Wu, X. Simulated-sunlight-activated photocatalysis of Methylene Blue using cerium-doped SiO₂/TiO₂ nanostructured fibers. *Journal of Environmental Sciences* **2012**, 24, 1867-1875, [https://doi.org/10.1016/S1001-0742\(11\)61008-5](https://doi.org/10.1016/S1001-0742(11)61008-5).
 22. Kokorin, A.I.; Sviridova, T.V.; Konstantinova, E.A.; Sviridov, D.V.; Bahnemann, D.W. Dynamics of Photogenerated Charge Carriers in TiO₂/MoO₃, TiO₂/WO₃ and TiO₂/V₂O₅ Photocatalysts with Mosaic

- Structure. *Catalysts* **2020**, *10*, 1022, <https://doi.org/10.3390/catal10091022>.
23. Liu, Z.; Wang, Q.; Tan, X.; Zheng, S.; Zhang, H.; Wang, Y.; Gao, S. Solvothermal preparation of Bi/Bi₂O₃ nanoparticles on TiO₂ NTs for the enhanced photoelectrocatalytic degradation of pollutants. *Journal of Alloys and Compounds* **2020**, *815*, 152478, <https://doi.org/10.1016/j.jallcom.2019.152478>.
 24. Jia, M.; Yang, Z.; Xu, H.; Song, P.; Xiong, W.; Cao, J.; Zhang, Y.; Xiang, Y.; Hu, J.; Zhou, C.; Yang, Y.; Wang, W. Integrating N and F co-doped TiO₂ nanotubes with ZIF-8 as photoelectrode for enhanced photoelectrocatalytic degradation of sulfamethazine. *Chemical Engineering Journal* **2020**, *388*, 124388, <https://doi.org/10.1016/j.cej.2020.124388>.
 25. Kim, M.W.; Joshi, B.; Samuel, E.; Seok, H.; Aldalbahi, A.; Almoqli, M.; Swihart, M.T.; Yoon, S.S. Electrosprayed MnO₂ on ZnO nanorods with atomic layer deposited TiO₂ layer for photoelectrocatalytic water splitting. *Applied Catalysis B: Environmental* **2020**, *271*, 118928, <https://doi.org/10.1016/j.apcatb.2020.118928>.
 26. Li, J.; Wang, J.; Huang, L.; Lu, G. Photoelectrocatalytic degradation of methyl orange over mesoporous film electrodes. *Photochemical & Photobiological Sciences* **2010**, *9*, 39–46, <https://doi.org/10.1039/B9PP00084D>.
 27. Çırak, B.B. Fabrication and characterization of transparent Cr-decorated TiO₂ nanoporous electrode for enhanced photo-electrocatalytic performance. *Vacuum* **2020**, *177*, 109375, <https://doi.org/10.1016/j.vacuum.2020.109375>.
 28. Shiprath, K.; Manjunatha, H.; Ratnam, K.V.; Janardhan, S.; Ratnamala, A.; Nadh, R.V.; Ramesh, S.; Naidu, K.C.B. Electrochemical study of anatase TiO₂ in aqueous sodium-ion electrolytes. *Biointerface Research in Applied Chemistry* **2020**, *10*, 5843–5848, <https://doi.org/10.33263/briac104.843848>.
 29. Davashloğlu, İ. Ç.; Özdokur, K.V.; Koçak, S.; Çırak, Ç.; Çağlar, B.; Çırak, B.B.; Ertaş, F.N. WO₃ decorated TiO₂ nanotube array electrode: Preparation, characterization and superior photoelectrochemical performance for rhodamine B dye degradation. *Journal of Molecular Structure* **2021**, *1241*, 130673, <https://doi.org/10.1016/j.molstruc.2021.130673>.
 30. del Barrio, M.; Rana, M.; Vilatela, J.J.; Lorenzo, E.; De Lacey, A.L.; Pita, M. Photoelectrocatalytic detection of NADH on n-type silicon semiconductors facilitated by carbon nanotube fibers. *Electrochimica Acta* **2021**, *377*, 138071, <https://doi.org/10.1016/j.electacta.2021.138071>.
 31. Navaee, A.; Salimi, A.; Sham, T.K. Bipolar electrochemistry as a powerful technique for rapid synthesis of ultrathin graphdiyne nanosheets: Improvement of photoelectrocatalytic activity toward both hydrogen and oxygen evolution. *International Journal of Hydrogen Energy* **2021**, *46*, 12906–12914, <https://doi.org/10.1016/j.ijhydene.2021.01.117>.
 32. Nurdin, M.; Arham, Z.; Rahayu, S.; Maulidiyah, M. Electroanalytical Performance of Graphene Paste Electrode Modified Al (III)-TiO₂ Nanocomposites in Fipronil Solution. *Jurnal Rekayasa Kimia & Lingkungan* **2020**, *15*(2), 71–78. <https://doi.org/10.23955/rkl.v15i2.16947>.
 33. Nurdin, M.; Maulidiyah, M.; Salim, L.O.A.; Muzakkar, M.Z.; Umar, A.A. High performance cypermethrin pesticide detection using anatase TiO₂-carbon paste nanocomposites electrode. *Microchemical Journal* **2019**, *145*, 756–761, <https://doi.org/10.1016/j.microc.2018.11.050>.
 34. Shi, J.; Qian, Q.; Jiang, H.; Li, H.; Wang, S.; Wei, F.; Feng, D. Effect of the Structure of Anodic TiO₂ Nanotube Arrays on Its Photoelectrocatalytic Activity. *Int. J. Electrochem. Sci* **2020**, *15*, 845–856, <https://doi.org/10.20964/2020.01.12>.
 35. Tsvetkov, N.; Larina, L.; Ku Kang, J.; Shevaleevskiy, O. Sol-gel processed TiO₂ nanotube photoelectrodes for dye-sensitized solar cells with enhanced photovoltaic performance. *Nanomaterials* **2020**, *10*, 296, <https://doi.org/10.3390/nano10020296>.
 36. Zhou, D.; Yu, B.; Chen, Q.; Shi, H.; Zhang, Y.; Li, D.; Yang, X.; Zhao, W.; Liu, C.; Wei, G.; Chen, Z. Improved visible light photocatalytic activity on Z-scheme g-C₃N₄ decorated TiO₂ nanotube arrays by a simple impregnation method. *Materials Research Bulletin* **2020**, *124*, 110757, <https://doi.org/10.1016/j.materresbull.2019.110757>.
 37. Dao, T.B.T.; Ha, T.T.L.; Do Nguyen, T.; Le, H.N.; Ha-Thuc, C.N.; Nguyen, T.M.L.; Perre, P.; Nguyen, D.M. Effectiveness of photocatalysis of MMT-supported TiO₂ and TiO₂ nanotubes for rhodamine B degradation. *Chemosphere* **2021**, *280*, 130802, <https://doi.org/10.1016/j.chemosphere.2021.130802>.
 38. Durdu, S.; Cihan, G.; Yalcin, E.; Altinkok, A. Characterization and mechanical properties of TiO₂ nanotubes formed on titanium by anodic oxidation. *Ceramics International* **2021**, *47*, 10972–10979, <https://doi.org/10.1016/j.ceramint.2020.12.218>.